Research Square

Preprints are preliminary reports that have not undergone peer review.
They should not be considered conclusive, used to inform clinical practice,
or referenced by the media as validated information.

A Complex-Quaternionic Riemann–Silberstein Formalism for Single-Photon Electromagnetic Wave Packets

Can Dogan Vurdu

cvurdu@kastamonu.edu.tr

Kastamonu University https://orcid.org/0000-0002-5179-1266

Zafer Ünal

Kastamonu University https://orcid.org/0000-0003-2445-1028

Research Article

Keywords: single photon, photon wave packet, Riemann–Silberstein vector, quaternionic Maxwell equation, helicity, quantum optics, quantized electromagnetic field, transition amplitude, mode matching, electromagnetic geometry

Posted Date: July 13th, 2026

DOI: https://doi.org/10.21203/rs.3.rs-10313172/v1

License: This work is licensed under a Creative Commons Attribution 4.0 International License.
Read Full License

Additional Declarations: The authors declare no competing interests.

A Complex-Quaternionic Riemann–Silberstein Formalism for Single-Photon Electromagnetic Wave Packets

Can Doğan Vurdu[1*]

Zafer Ünal[2]

[1]*Kastamonu University, Faculty of Engineering and Architecture, Department of Biomedical Engineering, 37100, Kastamonu, Türkiye*

[2]*Kastamonu University, Faculty of Sciences, Department of Mathematics, 37100, Kastamonu, Türkiye*

*Corresponding author: E mail: cvurdu@kastamonu.edu.tr

Abstract

Single photons are elementary excitations of the quantized electromagnetic field, yet their electromagnetic structure is often described through separate electric and magnetic field operators. Here we develop a theorem-based complex-quaternionic Riemann-Silberstein representation of single-photon electromagnetic wave packets. The formalism embeds the transverse electric and magnetic components into one helicity-resolved biquaternionic field, so that transversality, electric-magnetic orthogonality, helicity projection, and mode-wise nullity are encoded within a single algebraic structure. We show that the source-free Maxwell equations reduce to one first-order quaternionic Maxwell equation and that canonical quantization yields the one-photon electromagnetic amplitude as a vacuum-to-one-photon transition matrix element. The resulting expression is a spectral superposition of transverse modes weighted by the photon wave-packet envelope. Beyond notational compactness, the construction separates three operational ingredients of a one-photon state: spectral localization, helicity selection, and mode matching to a detector or target mode. The framework is fully compatible with standard QED and clarifies that broadband photon wave packets are generally not pointwise null, although each Fourier component is null.

Keywords: single photon; photon wave packet; Riemann–Silberstein vector; quaternionic Maxwell equation; helicity; quantum optics; quantized electromagnetic field; transition amplitude; mode matching; electromagnetic geometry

1. Introduction

The photon is the one-quantum excitation of the quantized electromagnetic field. In quantum optics, this statement is usually implemented by expanding the positive-frequency electric-field operator over transverse modes and associating creation and annihilation operators with those modes [1–4]. The magnetic field is then obtained from Maxwell's equations, or equivalently from the curl of the vector potential in a chosen gauge. This standard formulation is operationally successful, but it often hides a simple geometric fact: in free space, a radiation mode is not specified by an electric field alone. The magnetic field, propagation direction, and transversality constraint are tied together by a rigid cross-product structure.

A compact alternative is supplied by the Riemann–Silberstein (RS) representation, where the electric and magnetic fields are combined as

$$\mathbf{F}_{\pm} = \sqrt{\frac{\varepsilon_0}{2}}(\mathbf{E} \pm ic\mathbf{B}).$$

This representation has a long history in photon wave mechanics, including the Silberstein, Oppenheimer, Sipe, and Bialynicki-Birula formulations [5–9]. It has also become a practical tool in modern electromagnetic and light–matter calculations, where Maxwell's equations can be written in Schrödinger-like or helicity-resolved form [10,11]. The RS vector is particularly natural for photon energy-wave-function approaches because its squared norm is tied to electromagnetic energy density rather than to a Newton–Wigner position probability density [14,15].

Recent field-theoretic treatments of single photons emphasize that a single photon is detected discretely, while the quantum-field amplitude associated with it may possess a spatially extended wave-packet structure [16]. Related modern work on photon wave-packet mechanics uses helicity-resolved transverse fields and connects local wave equations to QED-level single-photon states [17]. In second quantization, the bridge between photon field operators and photon wave mechanics is commonly made by taking vacuum-to-one-photon matrix elements of positive-frequency field operators [18]. Many-mode one-photon states are also central in light–matter interaction, state transfer, single-photon absorption, and waveguide-QED scattering problems [19–22].

The present paper develops a complementary formulation. Instead of writing $\mathbf{E}$ and $\mathbf{B}$ as separate vector fields, we embed them in a complex-quaternionic, or biquaternionic, pure-vector field. This move is conservative: it does not replace complex Hilbert-space QED by a new quaternionic quantum theory in the sense of quaternionic Hilbert-space dynamics [23]. Quaternionic quantum mechanics and quaternionic wave-packet dynamics constitute a separate research direction [24]; here, by contrast, Hamilton's quaternion algebra is used only as a compact encoding of ordinary three-dimensional scalar and vector products. Throughout the paper, i denotes the commuting complex imaginary unit, whereas the quaternionic spatial basis units are denoted by $\mathbf{e}_1, \mathbf{e}_2, \mathbf{e}_3$. For two pure quaternions $\mathbf{a}$ and $\mathbf{b}$,

$$\mathbf{ab} = -\mathbf{a} \cdot \mathbf{b} + \mathbf{a} \times \mathbf{b}. \qquad (1)$$

Thus, the same algebraic product contains the dot-product constraint responsible for orthogonality and the cross-product relation that determines the magnetic component from the electric component and the propagation direction.

The paper's contribution is a theorem-proof formulation of the following statement: a single-photon electromagnetic wave packet may be represented as the vacuum-to-one-photon transition amplitude of a helicity-resolved biquaternionic Riemann–Silberstein field operator. The spectral envelope $f_\lambda(\mathbf{k})$ controls localization and mode matching, while the quaternionic helicity projector enforces the transverse electromagnetic geometry mode by mode. The result is not a new photon ontology and not a modification of quantum electrodynamics; it is a compact, algebraically transparent representation of standard free-space QED.

The novelty is therefore not the RS vector itself, nor the canonical one-photon Fock-state construction. The novelty is the systematic packaging of quaternionic vector algebra, helicity projectors, source-free Maxwell dynamics, and one-photon transition amplitudes into one theorem-level formalism. Compared with earlier RS photon-wave-function formulations, the present formalism adds two specific layers. First, the quaternionic product makes dot-product constraints and cross-product Maxwell relations appear in one multiplication rule. Second, the QED construction is stated directly as a field-operator transition amplitude, which avoids interpreting a one-photon Fock state as a classical electromagnetic field. This distinction is important in view of the photon-localization and photon-wave-function ambiguities discussed in the recent photon–classical-field literature [14,15].

Conceptual and operational significance. The present representation addresses a practical issue common to quantum optics, quantum field theory, and nanophotonics: how to discuss the electromagnetic content associated with a one-photon Fock excitation without replacing that excitation by a classical electromagnetic field. In the proposed formalism, the spectral function $f_\lambda(\mathbf{k})$ specifies the prepared or detected wave-packet mode, the helicity projector selects the circular-polarization sector, and the quaternionic product fixes the electric–magnetic geometry of each Fourier component. This makes the construction useful not only as an algebraic rewriting of Maxwell theory, but also as a compact operational language for single-photon preparation, phase shaping, absorption, and projection onto target modes.

Table 1 situates the present construction relative to standard QED, the Riemann–Silberstein representation, and photon wave-packet mechanics. It clarifies that the novelty of the present work is not the replacement of these established formalisms, but their compact theorem-level packaging through biquaternionic vector algebra, helicity projection, and vacuum-to-one-photon transition amplitudes.

Table 1. Relation of the present formalism to existing electromagnetic and photon wave-packet frameworks.

Formalism	Main object	Interpretation	Role in this paper
Standard QED	$\hat{\mathbf{E}}^{(+)}, \hat{\mathbf{B}}^{(+)}$	Field operators and Fock states	Starting point

Riemann–Silberstein representation	$\mathbf{F}_{\pm} = \sqrt{\varepsilon_0/2}(\mathbf{E} \pm ic\mathbf{B})$	Energy-amplitude / photon wave-function formalism	Field combination
Photon wave-packet mechanics	$f_\lambda(\mathbf{k})$, wave-packet modes	Spatial and spectral structure of one-photon states	Localization and mode matching
Present formalism	$\mathbb{F}_\eta$, P_η, $\Psi^{(+)}_{\eta,f}$	Biquaternionic transition-amplitude representation	Compact theorem-level packaging

The logical workflow of the construction is then shown in Figure 1.

This organization is intended to make the formal result readable across subfields: the upper level of the construction is standard field quantization, while the added biquaternionic layer only packages the transverse electromagnetic geometry and helicity selection in a single object.

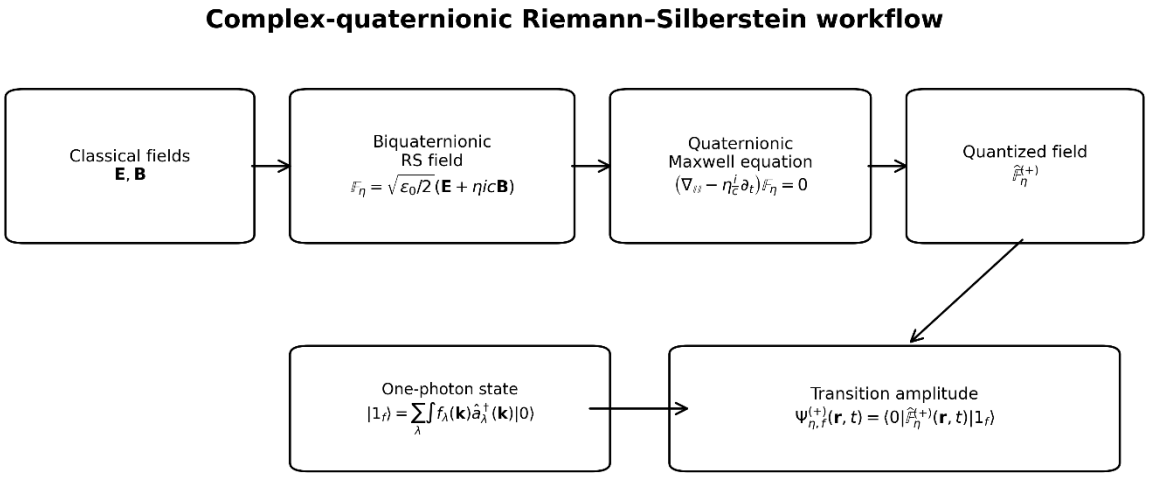


Figure 1. Conceptual structure of the complex-quaternionic Riemann-Silberstein representation. The electric and magnetic fields are first combined into the helicity-resolved biquaternionic field $\mathbb{F}_\eta$. The source-free Maxwell equations are then written as one first-order quaternionic equation. After canonical quantization, the corresponding positive-frequency field operator yields the single-photon electromagnetic wave-packet amplitude as the vacuum-to-one-photon transition matrix element.

2. Preliminaries: Complexified Quaternions and Pure-Vector Fields

Definition 2.1 (Complexified quaternions). Let $\mathbb{H}$ be the quaternion algebra with basis $1, \mathbf{e}_1, \mathbf{e}_2, \mathbf{e}_3$ satisfying

$$\mathbf{e}_i\mathbf{e}_j = -\delta_{ij} + \epsilon_{ijk}\mathbf{e}_k. \qquad (2)$$

The complexified quaternion algebra is

$$\mathbb{H}_{\mathbb{C}} = \mathbb{C} \otimes \mathbb{H}, \qquad (3)$$

where the ordinary complex unit i commutes with all quaternion units $\mathbf{e}_j$. Throughout this paper, repeated spatial indices are summed over 1,2,3.

Definition 2.2 (Pure quaternion representation of vectors). A three-vector $\mathbf{a} = (a_1, a_2, a_3)$, with real or complex components, is identified with the pure quaternion

$$\mathbf{a} = a_1\mathbf{e}_1 + a_2\mathbf{e}_2 + a_3\mathbf{e}_3. \qquad (4)$$

For

$$Q = q_0 + q_j\mathbf{e}_j \in \mathbb{H}_{\mathbb{C}},$$

define the scalar and vector parts as

$$\mathrm{Sc}(Q) = q_0, \qquad \mathrm{Vec}\,(Q) = q_j\mathbf{e}_j. \qquad (5)$$

Unless otherwise stated, the dot product for complex vector components is the complex bilinear Euclidean product, not the Hermitian inner product.

Lemma 2.3 (Quaternionic product identity). For pure quaternions $\mathbf{a}$ and $\mathbf{b}$,

$$\mathbf{ab} = -\mathbf{a}\cdot\mathbf{b} + \mathbf{a}\times\mathbf{b}. \qquad (6)$$

Consequently,

$$\mathrm{Sc}(\mathbf{ab}) = -\mathbf{a}\cdot\mathbf{b}, \qquad \mathrm{Vec}\,(\mathbf{ab}) = \mathbf{a}\times\mathbf{b}. \qquad (7)$$

Proof. Using $\mathbf{a} = a_i\mathbf{e}_i$, $\mathbf{b} = b_j\mathbf{e}_j$, and

$$\mathbf{e}_i\mathbf{e}_j = -\delta_{ij} + \epsilon_{ijk}\mathbf{e}_k,$$

we obtain

$$\mathbf{ab} = a_ib_j\mathbf{e}_i\mathbf{e}_j, \qquad (8)$$
$$\mathbf{ab} = -a_ib_j\delta_{ij} + a_ib_j\epsilon_{ijk}\mathbf{e}_k, \qquad (9)$$

and therefore

$$\mathbf{ab} = -\mathbf{a}\cdot\mathbf{b} + \mathbf{a}\times\mathbf{b}. \qquad (10)$$

This proves the result. □

Corollary 2.4 (Orthogonality as vanishing scalar part). For pure quaternions $\mathbf{a}$ and $\mathbf{b}$,

$$\mathbf{a} \perp \mathbf{b} \Leftrightarrow \mathrm{Sc}\,(\mathbf{ab}) = 0. \qquad (11)$$

Proof. By Lemma 2.3,

$$\mathrm{Sc}\,(\mathbf{ab}) = -\mathbf{a} \cdot \mathbf{b}.$$

The scalar part vanishes exactly when the dot product vanishes. □

Definition 2.5 (Quaternionic differential operator). Define

$$\nabla_{\mathbb{H}} = \mathbf{e}_1\,\partial_x + \mathbf{e}_2\,\partial_y + \mathbf{e}_3\,\partial_z. \qquad (12)$$

For a pure-vector field $\mathbf{V}(\mathbf{r}, t)$, the product rule gives

$$\nabla_{\mathbb{H}}\mathbf{V} = -\nabla \cdot \mathbf{V} + \nabla \times \mathbf{V}. \qquad (13)$$

Thus, the quaternionic differential operator simultaneously contains the divergence and curl of a vector field. In particular, if $\mathbf{V}$ is transverse, namely if

$$\nabla \cdot \mathbf{V} = 0,$$

then

$$\nabla_{\mathbb{H}}\mathbf{V} = \nabla \times \mathbf{V}.$$

This identity will be used below to rewrite the source-free Maxwell equations as a single first-order complex-quaternionic equation.

3. Quaternionic Riemann–Silberstein Field

Definition 3.1 (Helicity-resolved biquaternionic field). For real electromagnetic fields $\mathbf{E}$ and $\mathbf{B}$, define

$$\mathbb{F}_\eta(\mathbf{r}, t) = \sqrt{\frac{\varepsilon_0}{2}}\,[\mathbf{E}(\mathbf{r}, t) + \eta ic\mathbf{B}(\mathbf{r}, t)], \qquad \eta = \pm 1. \qquad (14)$$

The index η labels the two duality or helicity sectors.

Remark 3.2. The factor $\sqrt{\varepsilon_0/2}$ gives $\mathbb{F}_\eta$ the conventional Riemann–Silberstein energy-amplitude normalization. Nothing in the algebraic equivalence below depends on this numerical prefactor.

Theorem 3.3 (Source-free Maxwell equations as one quaternionic equation). Let $\mathbf{E}$ and $\mathbf{B}$ be sufficiently smooth real fields in a source-free vacuum region. Then the vacuum Maxwell equations

$$\nabla \cdot \mathbf{E} = 0, \qquad \nabla \cdot \mathbf{B} = 0, \qquad \nabla \times \mathbf{E} = -\partial_t \mathbf{B}, \qquad \nabla \times \mathbf{B} = \frac{1}{c^2}\partial_t \mathbf{E} \tag{15}$$

are equivalent to

$$\left(\nabla_{\mathbb{H}} - \eta \frac{i}{c}\partial_t\right) \mathbb{F}_\eta(\mathbf{r}, t) = 0 \tag{16}$$

for either choice $\eta = \pm 1$.

Proof. Using equation (13), we have

$$\nabla_{\mathbb{H}} \mathbb{F}_\eta = \sqrt{\frac{\varepsilon_0}{2}}[-\nabla \cdot \mathbf{E} - \eta i c \nabla \cdot \mathbf{B} + \nabla \times \mathbf{E} + \eta i c \nabla \times \mathbf{B}]. \tag{17}$$

The time-derivative term is

$$\eta \frac{i}{c}\partial_t \mathbb{F}_\eta = \sqrt{\frac{\varepsilon_0}{2}}\left[\eta \frac{i}{c}\partial_t \mathbf{E} - \partial_t \mathbf{B}\right], \tag{18}$$

because $\eta^2 = 1$ and $i^2 = -1$. Therefore,

$$\left(\nabla_{\mathbb{H}} - \eta \frac{i}{c}\partial_t\right) \mathbb{F}_\eta = 0$$

has scalar part

$$-\sqrt{\frac{\varepsilon_0}{2}}(\nabla \cdot \mathbf{E} + \eta i c \nabla \cdot \mathbf{B}) = 0. \tag{19}$$

Since $\mathbf{E}$ and $\mathbf{B}$ are real fields, the real and imaginary parts vanish separately. Hence,

$$\nabla \cdot \mathbf{E} = 0, \qquad \nabla \cdot \mathbf{B} = 0.$$

The vector part is

$$\nabla \times \mathbf{E} + \partial_t \mathbf{B} + \eta i \left(c \nabla \times \mathbf{B} - \frac{1}{c}\partial_t \mathbf{E}\right) = 0. \tag{20}$$

Separating real and imaginary parts gives

$$\nabla \times \mathbf{E} = -\partial_t \mathbf{B}, \qquad \nabla \times \mathbf{B} = \frac{1}{c^2}\partial_t \mathbf{E}.$$

Thus, the quaternionic equation implies the source-free Maxwell equations. Conversely, substituting the Maxwell equations in equation (15) into the same expression gives equation (16). This proves the equivalence. □

Corollary 3.4 (Wave equation). Each component of $\mathbb{F}_\eta$ satisfies the free wave equation

$$\left(\nabla^2 - \frac{1}{c^2}\partial_t^2\right)\mathbb{F}_\eta = 0. \qquad (21)$$

Proof. The Maxwell equations imply the wave equation for **E** and **B** separately. Since $\mathbb{F}_\eta$ is a linear combination of **E** and **B**, each component of $\mathbb{F}_\eta$ also satisfies the same free wave equation.

Equivalently, one may apply the conjugate first-order operator to equation (16). Since

$$\nabla_{\mathbb{H}}^2 = -\nabla^2,$$

the product of the two first-order operators gives

$$\left(\nabla^2 - \frac{1}{c^2}\partial_t^2\right)\mathbb{F}_\eta = 0.$$

This proves the result. □

4. Helicity Projection and Mode-Wise Electromagnetic Geometry

Let $\mathbf{k} \neq 0$, $\hat{\mathbf{k}} = \mathbf{k}/|\,\mathbf{k}\,|$, and $\omega_k = c\,|\,\mathbf{k}\,|$. The physical polarization space is the transverse plane

$$\mathcal{T}_{\mathbf{k}} = \{\mathbf{v} \in \mathbb{C}^3 : \hat{\mathbf{k}} \cdot \mathbf{v} = 0\}. \qquad (22)$$

The mode-wise transverse geometry is illustrated in Figure 2.

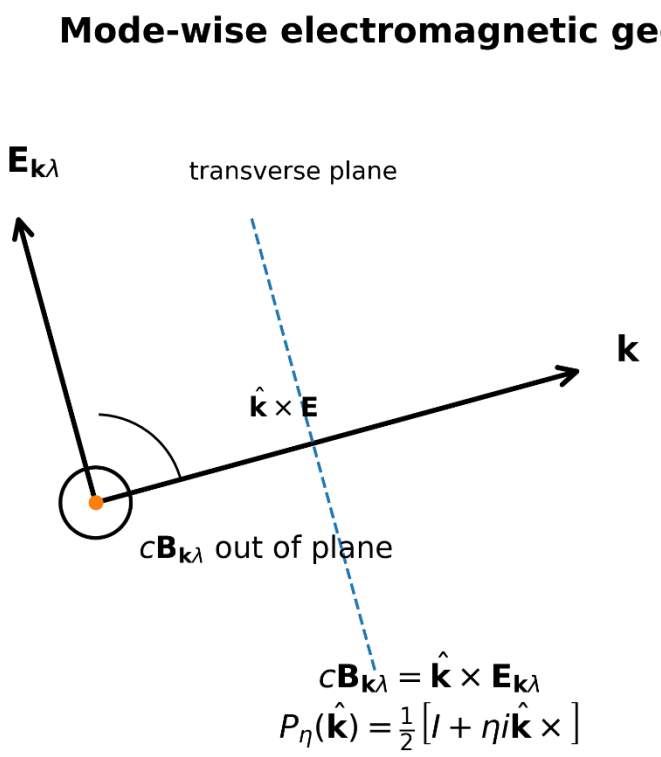


Figure 2. Mode-wise electromagnetic geometry enforced by the helicity projector. For each Fourier mode, the electric field, magnetic field, and propagation direction form a transverse triad satisfying $c\mathbf{B}_{\mathbf{k}\lambda} = \hat{\mathbf{k}} \times \mathbf{E}_{\mathbf{k}\lambda}$. The helicity projector $P_\eta(\hat{\mathbf{k}})$ selects the circular-polarization sector and enforces the electromagnetic geometry mode by mode.

Definition 4.1 (Helicity operator and projectors). On $\mathcal{T}_{\hat{\mathbf{k}}}$, define

$$H_{\hat{\mathbf{k}}}\mathbf{v} = i\hat{\mathbf{k}} \times \mathbf{v}, \qquad (23)$$

and

$$P_\eta(\hat{\mathbf{k}}) = \frac{1}{2}(I + \eta H_{\hat{\mathbf{k}}}), \eta = \pm 1. \qquad (24)$$

Lemma 4.2 (Helicity projector algebra). On $\mathcal{T}_{\hat{\mathbf{k}}}$,

$$H_{\hat{\mathbf{k}}}^2 = I, \quad P_\eta^2 = P_\eta, \quad P_+P_- = 0, \quad P_+ + P_- = I. \qquad (25)$$

Proof. For $\mathbf{v} \in \mathcal{T}_{\hat{\mathbf{k}}}$, the vector identity

$$\hat{\mathbf{k}} \times (\hat{\mathbf{k}} \times \mathbf{v}) = \hat{\mathbf{k}}(\hat{\mathbf{k}} \cdot \mathbf{v}) - \mathbf{v} = -\mathbf{v}$$

gives

$$H_{\hat{\mathbf{k}}}^2 \mathbf{v} = i^2 \hat{\mathbf{k}} \times \left(\hat{\mathbf{k}} \times \mathbf{v}\right) = \mathbf{v}. \qquad (26)$$

The projector relations then follow algebraically from $H_{\hat{\mathbf{k}}}^2 = I$. □

Theorem 4.3 (Plane-wave solutions and helicity selection). Let $\boldsymbol{\epsilon}_\lambda(\hat{\mathbf{k}}) \in \mathcal{T}_{\hat{\mathbf{k}}}$ be a circular polarization vector satisfying

$$i\hat{\mathbf{k}} \times \boldsymbol{\epsilon}_\lambda(\hat{\mathbf{k}}) = \lambda \boldsymbol{\epsilon}_\lambda(\hat{\mathbf{k}}), \lambda = \pm 1. \qquad (27)$$

For a positive-frequency plane wave with electric amplitude

$$\mathbf{E}_{\mathbf{k}\lambda}^{(+)}(\mathbf{r}, t) = \mathcal{E}_k \boldsymbol{\epsilon}_\lambda(\hat{\mathbf{k}}) e^{i(\mathbf{k}\cdot\mathbf{r} - \omega_k t)}, \qquad (28)$$

Maxwell's equations impose

$$c\mathbf{B}_{\mathbf{k}\lambda}^{(+)} = \hat{\mathbf{k}} \times \mathbf{E}_{\mathbf{k}\lambda}^{(+)}. \qquad (29)$$

The corresponding biquaternionic mode is

$$\mathbb{F}_{\eta,\mathbf{k}\lambda}^{(+)}(\mathbf{r}, t) = \sqrt{\frac{\varepsilon_0}{2}} \mathcal{E}_k \left[\boldsymbol{\epsilon}_\lambda(\hat{\mathbf{k}}) + \eta i \hat{\mathbf{k}} \times \boldsymbol{\epsilon}_\lambda(\hat{\mathbf{k}})\right] e^{i(\mathbf{k}\cdot\mathbf{r} - \omega_k t)}. \qquad (30)$$

Moreover,

$$\boldsymbol{\epsilon}_\lambda + \eta i \hat{\mathbf{k}} \times \boldsymbol{\epsilon}_\lambda = (1 + \eta\lambda)\boldsymbol{\epsilon}_\lambda, \qquad (31)$$

so $\mathbb{F}_\eta$ selects the helicity sector $\lambda = \eta$ and annihilates the opposite sector.

Proof. The Faraday equation for a positive-frequency plane wave gives

$$i\mathbf{k} \times \mathbf{E}^{(+)} = -\partial_t \mathbf{B}^{(+)} = i\omega_k \mathbf{B}^{(+)}. \qquad (32)$$

Hence,

$$c\mathbf{B}^{(+)} = \hat{\mathbf{k}} \times \mathbf{E}^{(+)}.$$

Substituting this relation into equation (14) gives equation (30). Finally, equation (27) gives equation (31). □

Corollary 4.4 (Mode-wise orthogonality). For every plane-wave mode satisfying equation (29),

$$\mathbf{k} \cdot \mathbf{E}_{\mathbf{k}\lambda} = 0, \qquad \mathbf{k} \cdot \mathbf{B}_{\mathbf{k}\lambda} = 0, \qquad \mathbf{E}_{\mathbf{k}\lambda} \cdot \mathbf{B}_{\mathbf{k}\lambda} = 0. \qquad (33)$$

Equivalently,

$$\mathbf{E}_{\mathbf{k}\lambda} \perp \mathbf{B}_{\mathbf{k}\lambda} \perp \mathbf{k}. \qquad (34)$$

Proof. The first condition is transversality. The second follows because

$$\mathbf{B} \propto \hat{\mathbf{k}} \times \mathbf{E},$$

which is orthogonal to $\hat{\mathbf{k}}$. The third follows from

$$\mathbf{E} \cdot \left(\hat{\mathbf{k}} \times \mathbf{E}\right) = 0.$$

In quaternionic language, these orthogonality statements are equivalent to vanishing scalar parts of the corresponding pure-quaternion products. □

Corollary 4.5 (Mode-wise null field). For a plane-wave radiation mode,

$$\mathbb{F}_\eta \cdot \mathbb{F}_\eta = 0, \qquad (35)$$

where the dot denotes the complex bilinear Euclidean product on vector components.

Equivalently,

$$\mathbf{E} \cdot \mathbf{B} = 0, \qquad |\,\mathbf{E}\,|^2 = c^2\,|\,\mathbf{B}\,|^2. \qquad (36)$$

Proof. From equation (14),

$$\mathbb{F}_\eta \cdot \mathbb{F}_\eta = \frac{\varepsilon_0}{2}(|\,\mathbf{E}\,|^2 - c^2\,|\,\mathbf{B}\,|^2 + 2\eta i c\mathbf{E} \cdot \mathbf{B}). \qquad (37)$$

A plane wave satisfies

$$\mathbf{E} \cdot \mathbf{B} = 0, \qquad |\,\mathbf{E}\,| = c\,|\,\mathbf{B}\,|,$$

and therefore the expression vanishes. □

5. Quantized Biquaternionic Field Operator

We now pass from classical modes to canonical QED. We work in free space with continuum normalization

$$\left[\hat{a}_\lambda(\mathbf{k}), \hat{a}^\dagger_{\lambda'}(\mathbf{k}')\right] = (2\pi)^3 \delta_{\lambda\lambda'} \delta^{(3)}(\mathbf{k} - \mathbf{k}'). \qquad (38)$$

The positive-frequency electric field operator is

$$\hat{\mathbf{E}}^{(+)}(\mathbf{r},t) = i\sum_{\lambda=\pm1}\int \frac{d^3k}{(2\pi)^3}\sqrt{\frac{\hbar\omega_k}{2\varepsilon_0}}\,\boldsymbol{\epsilon}_\lambda(\hat{\mathbf{k}})\hat{a}_\lambda(\mathbf{k})e^{i(\mathbf{k}\cdot\mathbf{r}-\omega_k t)}. \qquad (39)$$

The positive-frequency magnetic field operator is fixed by Maxwell's equations:

$$c\hat{\mathbf{B}}^{(+)}(\mathbf{r},t) = i\sum_{\lambda=\pm1}\int \frac{d^3k}{(2\pi)^3}\sqrt{\frac{\hbar\omega_k}{2\varepsilon_0}}\big[\hat{\mathbf{k}}\times\boldsymbol{\epsilon}_\lambda(\hat{\mathbf{k}})\big]\hat{a}_\lambda(\mathbf{k})e^{i(\mathbf{k}\cdot\mathbf{r}-\omega_k t)}. \qquad (40)$$

Definition 5.1 (Biquaternionic positive-frequency field operator). Define

$$\hat{\mathbb{F}}_\eta^{(+)}(\mathbf{r},t) = \sqrt{\frac{\varepsilon_0}{2}}\big[\hat{\mathbf{E}}^{(+)}(\mathbf{r},t) + \eta ic\hat{\mathbf{B}}^{(+)}(\mathbf{r},t)\big]. \qquad (41)$$

Equivalently,

$$\hat{\mathbb{F}}_\eta^{(+)}(\mathbf{r},t) = i\sum_{\lambda=\pm1}\int \frac{d^3k}{(2\pi)^3}\sqrt{\frac{\hbar\omega_k}{4}}\big[\boldsymbol{\epsilon}_\lambda(\hat{\mathbf{k}}) + \eta i\hat{\mathbf{k}}\times\boldsymbol{\epsilon}_\lambda(\hat{\mathbf{k}})\big]\hat{a}_\lambda(\mathbf{k})e^{i(\mathbf{k}\cdot\mathbf{r}-\omega_k t)}. \qquad (42)$$

Remark 5.2. The expectation value $\langle 1_f \mid \hat{\mathbf{E}} \mid 1_f\rangle$ of the electric field in a one-photon number state vanishes in the usual Fock-state sense. The object introduced below is therefore not a classical mean field. It is instead a vacuum-to-one-photon transition amplitude.

6. Single-Photon Wave-Packet Theorem

Definition 6.1 (One-photon wave packet). Let $f_\lambda(\mathbf{k})$ be square-integrable spectral amplitudes satisfying

$$\sum_{\lambda=\pm1}\int \frac{d^3k}{(2\pi)^3}|f_\lambda(\mathbf{k})|^2 = 1. \qquad (43)$$

The corresponding one-photon state is

$$\mid 1_f\rangle = \sum_{\lambda=\pm1}\int \frac{d^3k}{(2\pi)^3} f_\lambda(\mathbf{k})\hat{a}_\lambda^\dagger(\mathbf{k}) \mid 0\rangle. \qquad (44)$$

Theorem 6.2 (Biquaternionic single-photon transition amplitude). For the one-photon state in equation (44), the vacuum-to-one-photon transition amplitude of the biquaternionic field operator is

$$\Psi_{\eta,f}^{(+)}(\mathbf{r},t) = \langle 0 \mid \widehat{\mathbb{F}}_{\eta}^{(+)}(\mathbf{r},t) \mid 1_f \rangle, \qquad (45)$$

and is explicitly

$$\Psi_{\eta,f}^{(+)}(\mathbf{r},t) = i \sum_{\lambda=\pm 1} \int \frac{d^3k}{(2\pi)^3} \sqrt{\frac{\hbar\omega_k}{4}} f_\lambda(\mathbf{k}) \left[\boldsymbol{\epsilon}_\lambda(\hat{\mathbf{k}}) + \eta i \hat{\mathbf{k}} \times \boldsymbol{\epsilon}_\lambda(\hat{\mathbf{k}}) \right] e^{i(\mathbf{k}\cdot\mathbf{r} - \omega_k t)} . \qquad (46)$$

Proof. Substitute equations (42) and (44) into equation (45). The only nonzero vacuum matrix element is

$$\langle 0 \mid \hat{a}_\lambda(\mathbf{k}) \hat{a}_{\lambda'}^\dagger(\mathbf{k}') \mid 0 \rangle = (2\pi)^3 \delta_{\lambda\lambda'} \delta^{(3)}(\mathbf{k} - \mathbf{k}'), \qquad (47)$$

which collapses the primed integral and gives equation (46). □

Corollary 6.3 (Helicity-filtered form). If the polarization basis obeys equation (27), then

$$\Psi_{\eta,f}^{(+)}(\mathbf{r},t) = 2i \int \frac{d^3k}{(2\pi)^3} \sqrt{\frac{\hbar\omega_k}{4}} f_\eta(\mathbf{k}) \boldsymbol{\epsilon}_\eta(\hat{\mathbf{k}}) e^{i(\mathbf{k}\cdot\mathbf{r} - \omega_k t)} \, e^{i(\mathbf{k}\cdot\mathbf{r} - \omega_k t)}, \qquad (48)$$

where the opposite helicity component is projected out.

Proof. Apply equation (31) to equation (46). For $\lambda = \eta$, the bracket equals $2\boldsymbol{\epsilon}_\eta$; for $\lambda = -\eta$, it vanishes. □

Proposition 6.4 (Helicity-resolved energy norm). Assume that f_λ is normalized by equation (43) and has finite first frequency moment. For a helicity-filtered component, the transition amplitude satisfies

$$\int_{\mathbb{R}^3} d^3 r \, \Psi_{\eta,f}^{(-)}(\mathbf{r},t) \cdot \Psi_{\eta,f}^{(+)}(\mathbf{r},t) = \int \frac{d^3k}{(2\pi)^3} \hbar\omega_k \mid f_\eta(\mathbf{k}) \mid^2 , \qquad (49)$$

where $\Psi_{\eta,f}^{(-)} = \left[\Psi_{\eta,f}^{(+)} \right]^*$. Summing over $\eta = \pm 1$ gives the mean one-photon energy.

Proof. Using equation (48) and

$$\boldsymbol{\epsilon}_\eta^*(\hat{\mathbf{k}}) \cdot \boldsymbol{\epsilon}_\eta(\hat{\mathbf{k}}) = 1,$$

Parseval's identity gives

$$\int d^3 r \, \Psi_{\eta,f}^{(-)} \cdot \Psi_{\eta,f}^{(+)} = \int \frac{d^3k}{(2\pi)^3} \hbar\omega_k \mid f_\eta(\mathbf{k}) \mid^2 . \qquad (50)$$

The right-hand side is exactly the helicity-resolved expectation value of the free-field Hamiltonian in the one-photon state. The identity is an energy normalization, not a local photon-position probability normalization. □

Proposition 6.5 (Mode-matched single-photon projection). Let $| 1_g\rangle$ be another normalized one-photon wave packet with spectrum $g_\lambda(\mathbf{k})$. The ideal mode overlap is

$$\langle 1_g \mid 1_f\rangle = \sum_{\lambda=\pm1} \int \frac{d^3k}{(2\pi)^3} g_\lambda^*(\mathbf{k}) f_\lambda(\mathbf{k}) . \qquad (51)$$

An ideal detector or projector matched to g clicks with probability

$$| \langle 1_g \mid 1_f\rangle |^2$$

on the one-photon input $| 1_f\rangle$.

Proof. The result follows immediately from the canonical commutation relation in equation (38). Operationally, the packet envelope $f_\lambda(\mathbf{k})$ is therefore not only a localization function; it is also the object that determines mode matching in single-photon measurements. □

Theorem 6.6 (The transition amplitude satisfies the quaternionic Maxwell equation). Assume that $f_\lambda(\mathbf{k})$ is sufficiently regular so that differentiation may be interchanged with integration in equation (46). Then

$$\left(\nabla_{\mathbb{H}} - \eta \frac{i}{c}\partial_t\right) \Psi_{\eta,f}^{(+)}(\mathbf{r}, t) = 0. \qquad (52)$$

Proof. Each plane-wave integrand in equation (46) is a solution of the source-free quaternionic Maxwell equation by Theorems 3.3 and 4.3. Linearity and the assumed regularity permit the differential operator to pass through the integral, so the superposition is also a solution. □

Corollary 6.7 (Spectral localization versus spatial localization). A wave packet is localized by the spectral envelope $f_\lambda(\mathbf{k})$. For a Gaussian envelope centered at $\mathbf{k}_0$,

$$f_\lambda(\mathbf{k}) = C_\lambda \exp\left[-\frac{| \mathbf{k} - \mathbf{k}_0 |^2}{4\sigma_k^2}\right] e^{-i\mathbf{k}\cdot\mathbf{r}_0}, \qquad (53)$$

the transition amplitude is concentrated near $\mathbf{r}_0$ at $t = 0$, with approximate spatial width

$$\Delta x \sim \sigma_k^{-1}. \qquad (54)$$

Proof. The statement is the Fourier uncertainty relation applied to the spectral representation in equation (46). The phase factor in equation (53) translates the packet center to $\mathbf{r}_0$. The width estimate follows from the Fourier transform of a Gaussian. □

The role of the spectral envelope in spatial localization is shown schematically in Figure 3.

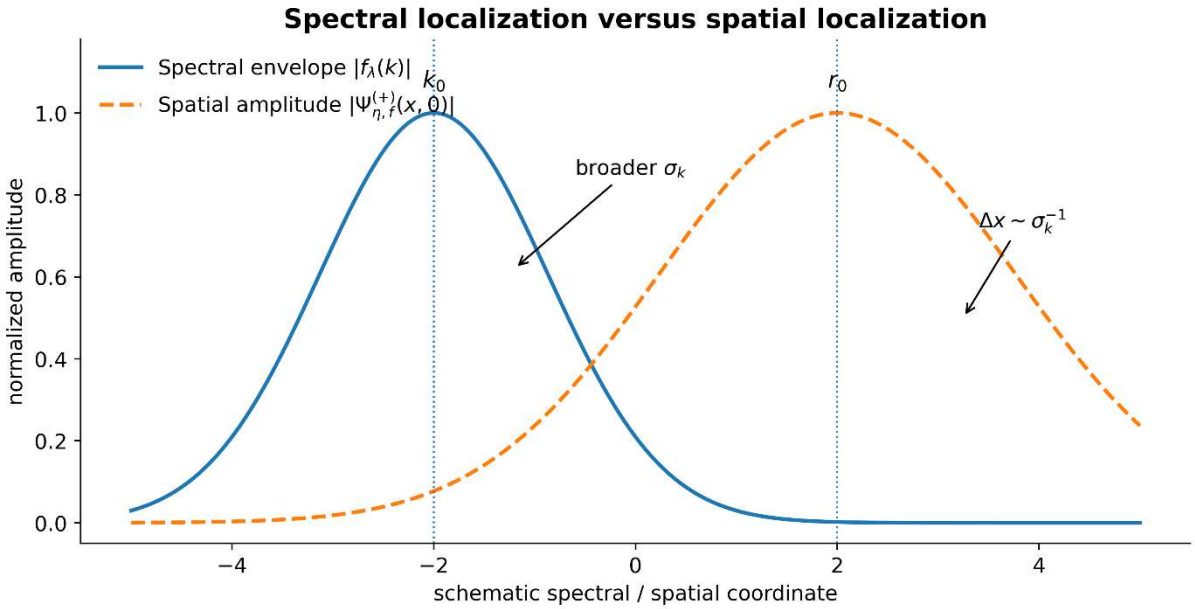


Figure 3. Spectral construction of a single-photon wave packet.

The spectral envelope $f_\lambda(\mathbf{k})$ determines the localization and mode content of the one-photon state. A Gaussian distribution centered at $\mathbf{k}_0$ produces a spatially concentrated transition amplitude near $\mathbf{r}_0$, with approximate width $\Delta x \sim \sigma_k^{-1}$. The quaternionic helicity factor fixes the electromagnetic geometry of each contributing mode.

7. Broadband Packets and the Null-Field Limitation

Proposition 7.1 (Mode-wise nullity does not imply pointwise packet nullity). Although each Fourier component in equation (46) is null in the sense of Corollary 4.5, the total broadband packet generally does not satisfy

$$\Psi^{(+)}_{\eta,f}(\mathbf{r},t) \cdot \Psi^{(+)}_{\eta,f}(\mathbf{r},t) = 0 \qquad (55)$$

at every space-time point.

Proof. Let

$$\Psi = \sum_n \Psi_n$$

denote a finite discrete superposition of null modes for clarity. Then

$$\Psi \cdot \Psi = \sum_n \Psi_n \cdot \Psi_n + 2 \sum_{m<n} \Psi_m \cdot \Psi_n. \qquad (56)$$

The first sum vanishes mode by mode, but the cross terms need not vanish when the modes have different propagation directions, phases, or polarizations. The same argument extends to the continuum by replacing the sum with a double integral. □

Corollary 7.2 (Paraxial or common-direction packets). If the support of $f_\lambda(\mathbf{k})$ is narrowly concentrated around a common propagation direction and a common helicity, then the packet is approximately null. The deviation from pointwise nullity is controlled by angular and spectral spread.

Proof. When all participating modes have nearly the same $\mathbf{k}$ and helicity, their polarization vectors and magnetic-field relations are nearly common. The cross terms in the proof of Proposition 7.1 then approach the same null cancellation as in a single mode. Corrections scale with the packet's angular and spectral spread. □

The difference between mode-wise nullity and packet-level nullity is summarized in Figure 4.

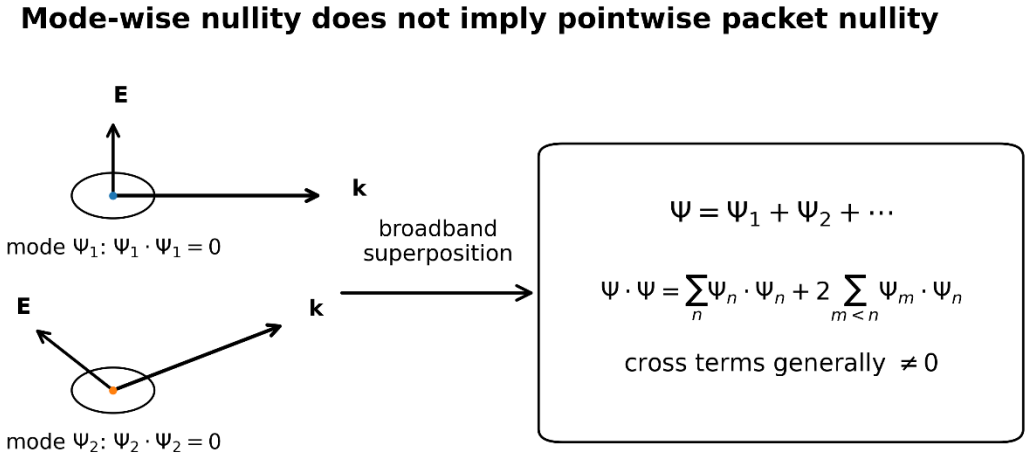


Figure 4. Mode-wise nullity versus packet-level nullity. Each individual plane-wave radiation mode is null, but a broadband superposition generally contains cross terms between different propagation directions, phases, or polarizations. Therefore, mode-wise nullity does not imply pointwise nullity of the total packet. Approximate null behavior is recovered in paraxial, common-direction, or common-helicity limits.

8. Interpretation and Relation to Standard QED

The state $|\, 1_f\rangle$ is an ordinary one-photon Fock state. The transition amplitude $\Psi^{(+)}_{\eta,f}$ is not a hidden classical electromagnetic field carried by a photon. It is a transition amplitude that gives a compact electromagnetic representation of the one-photon excitation. This distinction is essential because number states have vanishing first-order field expectation values, while transition amplitudes and correlation functions are nonzero and measurable through detection statistics.

The same caution appears in photon wave mechanics more generally: Riemann–Silberstein-based wave functions reproduce Maxwell-like evolution and energy-density amplitudes, but their coordinate-space scalar products and localization properties are subtler than those of massive nonrelativistic particles [14,15]. In the present construction, these subtleties are isolated in the spectral one-photon state and in the transition-amplitude interpretation.

The formalism has three useful separations:

(i) The spectral function $f_\lambda(\mathbf{k})$ determines the spatial and temporal wave-packet shape.

(ii) The helicity projector $P_\eta(\hat{\mathbf{k}})$ determines the circular-polarization sector.

(iii) The quaternionic product determines the mode-wise electromagnetic geometry,

$$\mathbf{E} \perp \mathbf{B} \perp \mathbf{k}.$$

This representation therefore preserves canonical QED while giving a compact notation for the electromagnetic content of a one-photon wave packet. It also supplies a natural bridge to Riemann–Silberstein photon wave mechanics and to helicity-spinor approaches, but without requiring a new quaternionic Hilbert-space postulate.

Operationally, this transition-amplitude viewpoint gives a direct route from a prepared spectrum $f_\lambda(\mathbf{k})$ to the electromagnetic amplitude probed by an ideal mode-matched measurement. The same object also identifies which helicity and transverse-field geometry couple to a target mode. In this sense, the formalism connects a field-theoretic Fock-state description to measurable single-photon operations such as wave-packet shaping, absorption by localized emitters, and projection onto arbitrary temporal or spatial modes.

9. Possible Extensions

The present paper treats free-space source-free propagation. Several experimentally and theoretically relevant extensions are natural:

(a) **Paraxial and angular-momentum beams.** The formalism may be specialized to Hermite–Gaussian, Laguerre–Gaussian, Bessel, or exact nonparaxial modes. Riemann–Silberstein methods are especially efficient for beams carrying angular momentum [12].

(b) **Structured media.** In dispersive, anisotropic, or inhomogeneous media, the simple free-space relation

$$c\mathbf{B} = \hat{\mathbf{k}} \times \mathbf{E}$$

must be replaced by the relevant modal relation. A medium-adapted version of the present construction could use numerical canonical quantization or macroscopic-QED modes [30,31].

(c) **Photon–source entanglement.** Source currents can label helicity components through their transverse Fourier components, as in QED-level photon-emission theory [17,18]. This

extension would connect the present free-field representation to microscopic emission processes and source-dependent photon wave packets.

(d) **Detection theory.** The transition amplitude can be connected to Glauber photodetection correlation functions and to POVM-based projection onto arbitrary single-photon packets [27]. In this setting, the spectral envelope $f_\lambda(\mathbf{k})$ determines both the wave-packet shape and the mode matching between the incoming photon and the detector.

(e) **Engineered Gaussian packets.** Gaussian single-photon envelopes may be linked to cavity-QED generation and waveguide-QED scattering models [22,28]. This would provide a practical setting in which the spectral envelope, helicity sector, and spatial localization can be controlled simultaneously.

(f) **Wave-packet shaping and hybrid excitations.** Phase-shaped single-photon packets, photon-added coherent states, and photon-to-surface-plasmon transfer provide possible settings where a compact electromagnetic-amplitude representation may be useful [29,32,33].

10. Conclusion

We have formulated a complex-quaternionic Riemann–Silberstein representation of single-photon electromagnetic wave packets. The central helicity-resolved field

$$\mathbb{F}_\eta = \sqrt{\frac{\varepsilon_0}{2}}\,(\mathbf{E}+\eta i c\mathbf{B}) \qquad (57)$$

satisfies the source-free first-order quaternionic Maxwell equation

$$\left(\nabla_{\mathbb{H}} - \eta\,\frac{i}{c}\,\partial_t\right)\mathbb{F}_\eta = 0. \qquad (58)$$

The helicity projector

$$P_\eta(\hat{\mathbf{k}}) = \frac{1}{2}\left[I + \eta i\hat{\mathbf{k}}\times\right] \qquad (59)$$

selects the desired circular-polarization sector and enforces the correct electric–magnetic cross-product structure for each Fourier mode. At the QED level, the single-photon electromagnetic wave-packet amplitude is introduced as the vacuum-to-one-photon transition matrix element

$$\Psi^{(+)}_{\eta,f}(\mathbf{r},t) = \langle 0 \mid \widehat{\mathbb{F}}^{(+)}_\eta(\mathbf{r},t) \mid 1_f\rangle, \qquad (60)$$

which evaluates to a helicity-projected superposition of transverse electromagnetic modes. The spectral envelope $f_\lambda(\mathbf{k})$ controls localization and mode matching, while the quaternionic-helicity factor fixes the mode-wise electromagnetic geometry.

The resulting formalism is compact, theorem-level, and conservative. It does not introduce a new photon ontology, nor does it replace standard QED. Rather, it provides an algebraically

transparent representation of the electromagnetic content of a one-photon Fock excitation. The construction also clarifies an important limitation: although each Fourier component is a null radiation mode, a broadband superposition is not generally pointwise null unless additional paraxial, common-direction, or common-helicity conditions are imposed.

Funding

No funding was received for this study.

Data availability

No experimental data were generated or analyzed in this study. The manuscript is theoretical. Any symbolic or numerical supplementary files can be generated from the equations provided in the text.

Code availability

The Python scripts used to generate the schematic figures are available from the corresponding author upon reasonable request. No custom numerical data-processing code is required to reproduce the theoretical derivations.

Competing interests

The authors declare no competing financial or personal interests.

Author contributions

Can Doğan Vurdu: Conceptualization, theoretical formulation, methodology, formal analysis, writing – original draft, visualization, and manuscript preparation.

Zafer Ünal: Methodology, theoretical discussion, formal analysis, validation, writing – review and editing, and manuscript revision.

Appendix A. Sign Conventions

The convention used throughout this paper is

$$i\hat{\mathbf{k}} \times \boldsymbol{\epsilon}_\lambda = \lambda \boldsymbol{\epsilon}_\lambda. \qquad \text{(A.1)}$$

Some optics texts adopt the opposite convention for labeling right- and left-handed circular polarization. Under that convention, the symbol λ is replaced by $-\lambda$. The physical projector remains unchanged once the helicity labels are adjusted:

$$P_\eta(\hat{\mathbf{k}}) = \frac{1}{2}\left[I + \eta i\hat{\mathbf{k}} \times\right].$$

Thus, the sign convention affects only the labeling of the two circular-polarization sectors, not the projector algebra or the physical content of the construction.

Appendix B. Relation Between Quaternionic Multiplication and Matrix Spin-One Notation

The helicity operator used in this paper is $H_{\hat{\mathbf{k}}} = i\hat{\mathbf{k}}\times$. It is equivalent to the spin-one generator projected along the propagation direction, up to the sign convention used for the spin-one matrices. With the convention

$$(S_j)_{mn} = -i\epsilon_{jmn},$$

one obtains

$$(S\cdot\hat{\mathbf{k}})\mathbf{v} = i\hat{\mathbf{k}}\times\mathbf{v}. \qquad \text{(B.1)}$$

Therefore,

$$H_{\hat{\mathbf{k}}} = S\cdot\hat{\mathbf{k}}$$

under this spin-matrix convention. If the opposite convention for S_j is used, the sign of this relation is reversed. This sign convention does not affect the helicity projector algebra, because the projectors are defined consistently with the chosen helicity labels.

Appendix C. Compact Theorem Map

The logical structure of the construction can be summarized as follows:

Quaternion product ⟶ Biquaternionic RS field ⟶ Quaternionic Maxwell equation

$$\mathbf{ab} = -\mathbf{a}\cdot\mathbf{b} + \mathbf{a}\times\mathbf{b}$$

$$\mathbb{F}_\eta = \sqrt{\frac{\varepsilon_0}{2}}(\mathbf{E}+\eta ic\mathbf{B})$$

$$\left(\nabla_{\mathbb{H}} - \eta\frac{i}{c}\partial_t\right)\mathbb{F}_\eta = 0.$$

At the quantum level, the positive-frequency biquaternionic field operator gives the single-photon transition amplitude

$$\Psi^{(+)}_{\eta,f} = \langle 0 \mid \widehat{\mathbb{F}}^{(+)}_\eta \mid 1_f\rangle,$$

while the spectral envelope

$$f_\lambda(\mathbf{k})$$

controls localization and mode matching.

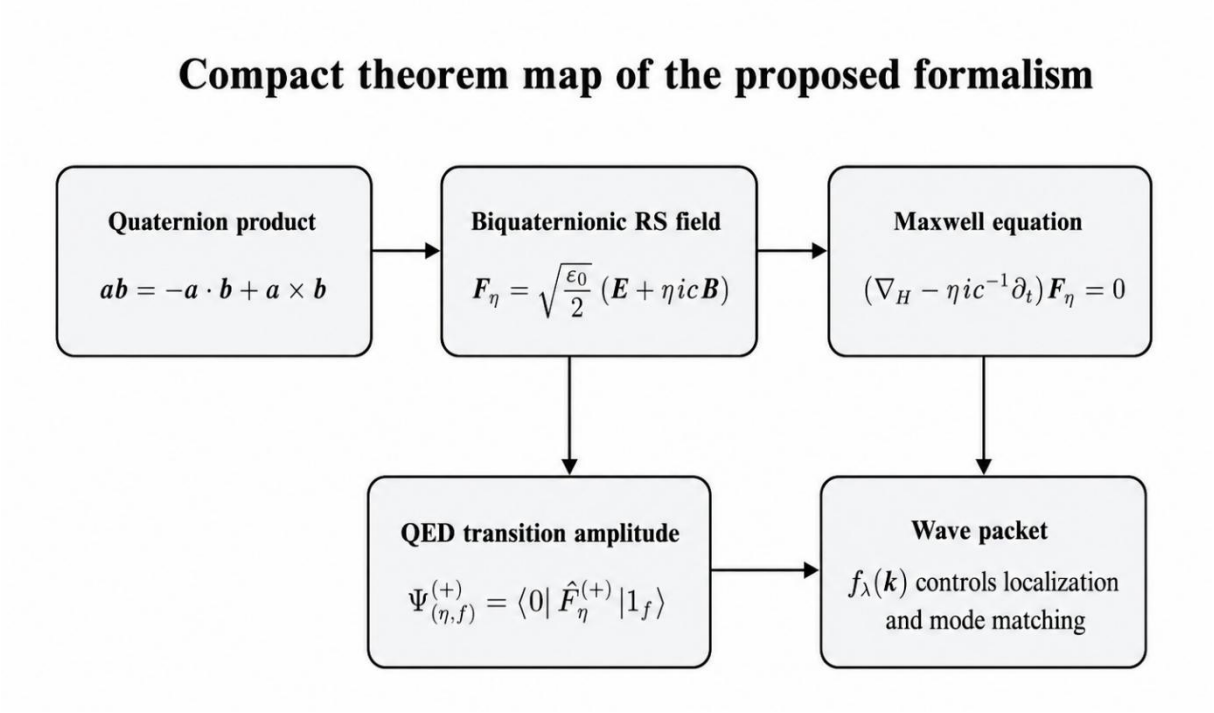


Figure C.1. Compact theorem map of the proposed formalism. The quaternion product first encodes scalar and vector products in a single algebraic rule. This structure is used to define the helicity-resolved biquaternionic Riemann–Silberstein field, which satisfies a first-order quaternionic Maxwell equation. After canonical quantization, the corresponding positive-frequency field operator yields the vacuum-to-one-photon transition amplitude, while the spectral envelope controls localization and mode matching.

References

[1] R. J. Glauber, Coherent and incoherent states of the radiation field, Physical Review 131 (1963) 2766--2788. https://doi.org/10.1103/PhysRev.131.2766.

[2] L. Mandel and E. Wolf, Optical Coherence and Quantum Optics, Cambridge University Press, 1995.

[3] C. Cohen-Tannoudji, J. Dupont-Roc and G. Grynberg, Photons and Atoms: Introduction to Quantum Electrodynamics, Wiley, 1997.

[4] R. Honegger and A. Rieckers, Construction of classical and non-classical coherent photon states, Annals of Physics 289 (2001) 213--231. https://doi.org/10.1006/aphy.2000.6128.

[5] L. Silberstein, Elektromagnetische Grundgleichungen in bivectorieller Behandlung, Annalen der Physik 327 (1907) 579--586. https://doi.org/10.1002/andp.19073270313.

[6] J. R. Oppenheimer, Note on light quanta and the electromagnetic field, Physical Review 38 (1931) 725--746. https://doi.org/10.1103/PhysRev.38.725.

[7] J. E. Sipe, Photon wave functions, Physical Review A 52 (1995) 1875--1883. https://doi.org/10.1103/PhysRevA.52.1875.

[8] I. Bialynicki-Birula, On the wave function of the photon, Acta Physica Polonica A 86 (1994) 97--116. https://doi.org/10.12693/APhysPolA.86.97

[9] I. Bialynicki-Birula, Photon wave function, in: E. Wolf (Ed.), Progress in Optics, Vol. 36, Elsevier, 1996, pp. 245--294. https://doi.org/10.1016/S0079-6638(08)70316-0.

[10] I. Bialynicki-Birula and Z. Bialynicka-Birula, The role of the Riemann-Silberstein vector in classical and quantum theories of electromagnetism, Journal of Physics A: Mathematical and Theoretical 46 (2013) 053001. https://doi.org/10.1088/1751-8113/46/5/053001.

[11] R. Jestaedt, M. Ruggenthaler, M. J. T. Oliveira, A. Rubio and H. Appel, Light-matter interactions within the Ehrenfest–Maxwell–Pauli–Kohn–Sham framework: fundamentals, implementation, and nano-optical applications. Advances in Physics, 68(4) (2019), 225–333. https://doi.org/10.1080/00018732.2019.1695875

[12] I. Bialynicki-Birula and Z. Bialynicka-Birula, Beams of electromagnetic radiation carrying angular momentum: the Riemann-Silberstein vector and the classical-quantum correspondence, Optics Communications, 264(2) (2006), 342-351. https://doi.org/10.1016/j.optcom.2005.11.071

[13] O. Keller, Space-time description of photon emission from an atom, Physical Review A 62 (2000) 022111. https://doi.org/10.1103/PhysRevA.62.022111.

[14] B. J. Smith and M. G. Raymer, Photon wave functions, wave-packet quantization of light, and coherence theory, New Journal of Physics 9 (2007) 414. https://doi.org/10.1088/1367-2630/9/11/414.

[15] D. Dragoman, On the photon-classical electromagnetic field relationship, Annals of the New York Academy of Sciences 1549 (2025) 11--21. https://doi.org/10.1111/nyas.15378.

[16] A. Aiello, Quantum field theory of single-photon states, Journal of Optics 27 (2025) 065201. https://doi.org/10.1088/2040-8986/addc7b.

[17] J. Jung and O. Keller, Local dynamical theory of two-spinor photon wave-packet mechanics and QED based on the transverse vector potential, Journal of Physics B: Atomic, Molecular and Optical Physics 59 (2026) 115503. https://doi.org/10.1088/1361-6455/ae768a.

[18] O. Keller, Quantum Theory of Near-Field Electrodynamics, Nano-Optics and Nanophotonics, Springer, 2011, Chapter 26. https://doi.org/10.1007/978-3-642-17410-0_26.

[19] M. Stobinska, G. Alber and G. Leuchs, Quantum electrodynamics of one-photon wave packets, arXiv:1002.3059 (2010).

[20] Y. Chen, M. Wubs, J. Mork and A. F. Koenderink, Coherent single-photon absorption by single emitters coupled to one-dimensional nanophotonic waveguides, New Journal of Physics 13 (2011) 103010. https://doi.org/10.1088/1367-2630/13/10/103010.

[21] D. Valente, F. Brito and T. Werlang, Dynamic Stark shift induced by a single photon packet, Opt. Lett. 42, (2017), 1692-1695. https://doi.org/10.1364/OL.42.001692

[22] O. A. Chuikin, Y. S. Greenberg, A. A. Shtygashev and A. G. Moiseev, Single-photon stimulated emission in waveguide quantum electrodynamics, European Physical Journal B 97 (2024) 159. https://doi.org/10.1140/epjb/s10051-024-00784-3.

[23] S. L. Adler, Quaternionic Quantum Mechanics and Quantum Fields, Oxford University Press, 1995.

[24] S. De Leo and G. C. Ducati, Quaternionic wave packets, J. Math. Phys. 48 (5), (2007), 052111. https://doi.org/10.1063/1.2738362

[25] W. R. Hamilton, Elements of Quaternions, Longmans, Green, and Co., 1866.

[26] J. B. Kuipers, Quaternions and Rotation Sequences: A Primer with Applications to Orbits, Aerospace, and Virtual Reality, Princeton University Press, 1999.

[27] T. B. Propp and S. J. van Enk, How to project onto an arbitrary single-photon wavepacket, Phys. Rev. A 102, (2020) 053707. https://doi.org/10.1103/PhysRevA.102.053707

[28] T. Utsugi, A. Goban, Y. Tokunaga, H. Goto and T. Aoki, Gaussian-wave-packet model for single-photon generation based on cavity quantum electrodynamics under adiabatic and nonadiabatic conditions, Phys. Rev. A 106, (2022), 023712. https://doi.org/10.1103/PhysRevA.106.023712

[29] H. P. Specht, J. Bochmann, M. Mucke, B. Weber, E. Figueroa, D. L. Moehring and G. Rempe, Phase shaping of single-photon wave packets, Nature Photon 3, (2009), 469–472. https://doi.org/10.1038/nphoton.2009.115

[30] D.-Y. Na, J. Zhu, W. C. Chew and F. L. Teixeira, Quantum information propagation preserving computational electromagnetics, Phys. Rev. A 102, (2020), 013711. https://doi.org/10.1103/PhysRevA.102.013711

[31] J. Feist, A. I. Fernandez-Dominguez and F. J. Garcia-Vidal, Macroscopic QED for quantum nanophotonics: emitter-centered modes as a minimal basis for multiemitter problems, Nanophotonics 10 (2020) 477--489. https://doi.org/10.1515/nanoph-2020-0451.

[32] M. S. Tame, C. Lee, J. Lee, D. Ballester, M. Paternostro, A. V. Zayats and M. S. Kim, Single-photon excitation of surface plasmon polaritons, Physical Review Letters 101 (2008) 190504. https://doi.org/10.1103/PhysRevLett.101.190504.

[33] A. Zavatta, S. Viciani and M. Bellini, Quantum-to-classical transition with single-photon-added coherent states of light, Science 306 (2004) 660--662. https://doi.org/10.1126/science.1103190.